Available online at www.sciencedirect.com

ScienceDirect

Procedia Structural Integrity 13 (2018) 1834–1839

Structural Integrity Procedia

www.elsevier.com/locate/procedia

ECF22 - Loading and Environmental effects on Structural Integrity

The corrosion resistance in artificial saliva of titanium and Ti-13Nb-13Zr alloy processed by high pressure torsion

Dragana Barjaktarević[1*], Jelena Bajat[1], Ivana Cvijović-Alagić[2], Ivana Dimić[1], Anton Hohenwarter[3], Veljko Đokić[1] and Marko Rakin[1]

[1]Faculty of Technology and Metallurgy, University of Belgrade, Belgrade, Serbia
[2]Institute of Nuclear Sciences ''Vinča'', University of Belgrade, Belgrade, Serbia
[3]Department of Materials Physics, Montanuniversität Leoben, Leoben, Austria

Abstract

In order to optimize and enhance the implant material properties, metallic materials may be modified by severe plastic deformation (SPD) procedures. One of the most attracting SPD methods is high-pressure torsion (HPT), which is method where deformation is obtained mainly by simple shear. In the present study ultrafine-grained titanium (UFG cpTi) and ultrafine-grained Ti-13Nb-13Zr (UFG TNZ) alloy were obtained by high pressure torsion (HPT) under a pressure of 4.1 GPa with a rotational speed of 0.2 rpm up to 5 rotations at room temperature. In order to analyse microstructure of materials before and after HPT process, scanning electron microscope (SEM) was used. The aim of this study was to determine the corrosion resistance of titanium and its alloy after HPT process. Electrochemical measurements were performed in artificial saliva with a pH value of 5.5 at 37°C, in order to simulate the oral environment. The materials were analysed by electrochemical impedance spectroscopy (EIS) and potentiodynamic polarization. All examined materials showed good corrosion resistance, but results indicate that HPT process can improves corrosion resistance.

Peer-review under responsibility of the ECF22 organizers.

Keywords: corrosion resistance, biomaterials, high pressure torsion, titanium alloy

1. Introduction

The good corrosion resistance is important properties for metallic biomaterials, because the ion release from the implant to the surrounding tissue may give rise to problems in the human body [1]. Titanium and its alloy show very good corrosion resistance in many media due to the formation of passive TiO_2 thin film on its surface [2]. The cpTi is one of the best metallic biomaterial for dental application due to corrosion resistance, but it does not have high enough strength for more applications. The mechanical properties of metallic biomaterials may be improved by severe plastic deformation (SPD) procedures, which lead to the formation of ultra fine microstructures.

* Dragana R. Barjaktarević. Tel.: +381-63-546-596.
*E-mail address:*dbarjaktarevic@tmf.bg.ac.rs.

2452-3216
Peer-review under responsibility of the ECF22 organizers.
10.1016/j.prostr.2018.12.332

A large number of different SPD methods exist, such as equal channel angular pressing (ECAP), high pressure torsion (HPT) and others similar processes [3]. High pressure torsion (HPT) is SPD method where deformation is obtained mainly by simple shear. The HPT process is shown in Figure 1. This method applies very large strains in a material due to the applied hydrostatic pressure during deformation and can make obtaining small grains and high strength possible, without larger changes in the sample dimension [4]. An equivalent strain (ε) imposed on the sample can be estimated using the formula [3]:

$$\varepsilon = \frac{2\pi Nr}{\sqrt{3}t} \tag{1}$$

As can be seen, the equivalent strain depends on the number of rotations (N), the radius (r) and the thickness (t) of the sample obtained by HPT process. Ultrafine-grained (UFG) metals and alloys produced by severe plastic deformation (SPD) techniques have better mechanical and physical properties compared to their coarse-grained (CG) counterparts [5-7].

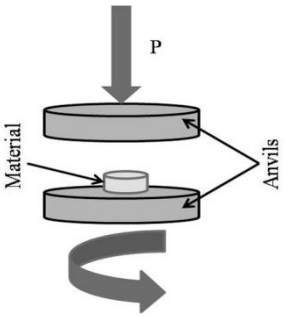

Fig. 1 Schematic representation of the HPT process

2. Material and Methods

The commercially pure titanium (CG cpTi) and Ti-13Nb-13Zr alloy (CG TNZ) were cut into disc-shape samples with a diameter of 28 mm and thickness of 2.26 mm. The one group of commercially pure titanium (CG cpTi) and Ti-13Nb-13Zr (CG TNZ) alloy samples were subjected to HPT process in order to obtain ultrafine grained commercially pure titanium (UFG cpTi) and Ti-13Nb-13Zr (UFG TNZ) alloy. High-pressure torsion process (HPT) was performed at room temperature, with applied pressure of 4.1 GPa, with a rotational speed of 0.2 rpm up to 5 rotations. The obtained samples were disc-shaped with a diameter of 34 mm and thickness of approximately 1.70 mm. In order to analyze characteristics of the microstructure scanning electron microscope (SEM) MIRA3 TESCAN was used. Electrochemical measurements were carried out on the cp Ti and TNZ alloy before and after HPT process. The electrolyte was an artificial saliva solution (The Pharmacy Belgrade, Serbia) in order to simulate the oral environment. The samples were immersed in artificial saliva with pH value of 5.5 at 37±1 ^{0}C. Fresh solution was used for each experiment. After surface preparation, each sample was immersed into an artificial saliva solution for 30 min to achieve a steady open - circuit potential (E_{OCP}). Electrochemical measurements were performed using a Gamry Reference 600 potentiostat within a Faraday cage. Electrochemical impedance spectroscopy (EIS) measurements were performed at OCP over a frequency range from 0.01 to 100000 Hz using sinusoidal AC voltage amplitude of ±10 mV. Potentiodynamic polarization was carried out in the potential ranging between -1 V to 4 V with respect to the OCP at a scan rate of 1.0 mVs^{-1}. In order to maintain a high statistical accuracy, electrochemical measurements were repeated at least three times.

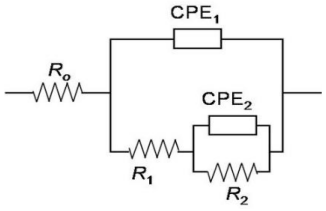

Fig. 2 The equivalent circuit of the examined materials in electrochemical tests

3. Results and Discussion

3.1 Microstructure characterization

The characteristic microstructure of the cp Ti (CG and UFG) and TNZ alloy (CG and UFG) are shown in SEM images in Fig. 3. Figure 3a shows cpTi microstructure after HPT process. The HPT process progressively leads to the transformation of the initial structure of the cpTi into a new ultrafine structure upon continued straining. The figure 3b shows that the microstructure of Ti–13Nb–13Zr alloy consists of acicular martensitic α', which is embedded in β phase. HPT microstructure is substantially different from the initial structure, acicular martensitic morphology microstructure is not noticeable. Grain refinement is preformed during the HPT, which is manifested by the appearance of globular grains and sub grains. Size of grains depends on the conditions of the HPT process. Dimić et al. [8] revealed that the microstructure of these materials are sufficiently homogeneous after HPT deformation under a pressure of 7.8 GPa up to 5 rotations at room temperature. Sharman et al. [9] shows that the HPT process after 50 turns shows homogenous microstructure with diameters ranging of grains from 20 to 50 nm, while 1 turn shows inhomogeneous microstructure with larger grains.

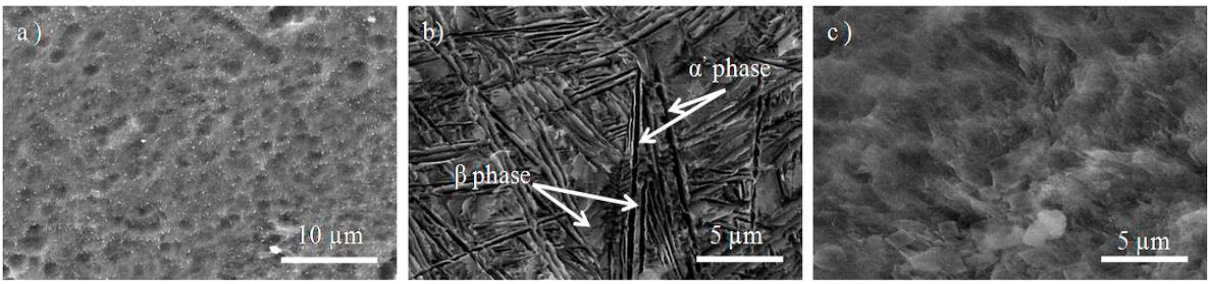

Fig. 3 SEM micrographs showing the microstructure of the examined materials: (a) UFG cpTi, (b) CG TNZ, (c) UFG TNZ

3.2 Corrosion resistance measurement

The polarization curves for the analyzed materials in artificial saliva, pH 5.5, are shown in Fig. 4. The materials corrosion resistance could be determined based on its corrosion current density, j_{corr}, so that the lower value of j_{corr} value suggests higher corrosion resistant material. The corrosion potential, E_{corr}, and corrosion current density, j_{corr}, determined for all samples from Fig. 4, are presented in Table 1. The small j_{corr} values for all analyzed materials, of the order of magnitude ranging from 10^{-6} – 10^{-9}A cm^{-2}, suggest their excellent corrosion resistance.

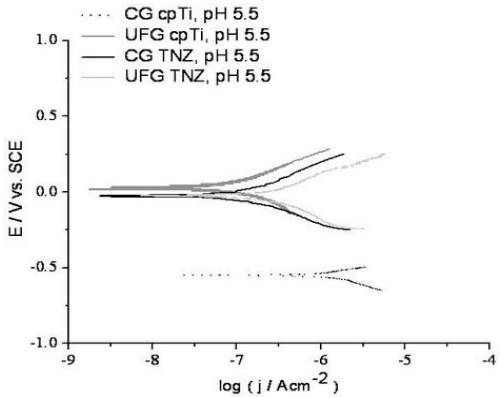

Fig. 4 The potentiodynamic polarization curves of analyzed materials

As can be seen from diagrams presented in Fig.4 and in Table 1, j_{corr} is higher for CG cpTi compared to UFG cpTi. The HPT process performed on the commercially pure titanium improved corrosion resistance. Namely, UFG cpTi after HPT process showed the lowest j_{corr} value (67.6 nAcm^{-2}), which is almost fourteen times lower than j_{corr} value for CG cpTi (955 nAcm^{-2}). On the other hand, UFG TNZ alloy showed lower corrosion resistance than CG TNZ

alloy. This result indicates that HPT process did not improve corrosion resistance of the alloy. Namely, UFG TNZ alloy showed the slightly higher j_{corr} value (166 nAcm^{-2}), than j_{corr} value for CG TNZ alloy (103 nAcm^{-2}). Also, CG TNZ alloy shows higher corrosion resistance than cpTi. This happens due to zirconium, which leads to better corrosion resistance [10].

Table 1. Electrochemical parameters of materials

Material	CG cpTi	UFG cpTi	CG TNZ	UFG TNZ
E_{corr} (V)	-0.56	0.023	-0.028	-0.024
j_{corr} (nA/cm^2)	955	67.6	103	166

The Nyquist plot for the examined materials in artificial saliva with pH value of 5.5 were shown in Figure 5, while the Bode plots was shown in Figure 6. As can be seen in Figure 5, Z_{imag} and Z_{real} values for UFG cpTi are higher than that of CG cpTi. Therefore, it can be concluded that cpTi had less corrosion resistance than UFG cpTi. On the other hand, figure 5 shows that Z_{imag} and Z_{real} values for UFG TNZ are lower than that of CG TNZ, which indicated lower corrosion resistance for alloy after HPT process.

Furthermore, the total impedance value for the UFG cpTi is higher than that of the CG cpTi, while UFG TNZ alloy has lower the total impedance value than CG TNZ alloy according to Bode plots, Figure 6. The Bode plots showed two time constants, which correspond to two interfaces. The time constant at high frequencies (R_1CPE_1) corresponds to the outer porous layer, while the time constant at low frequencies (R_2CPE_2) is related to high corrosion resistant inner barrier layer [11]. The EIS data were successfully fit by equivalent circuit shown (EEC) in Figure 2. R_s represents the solution resistance. The agreement between experimental and simulated results was evaluated by "Goodness of Fit" parameter and values of the order 10^{-3}, indicated a good fitting.

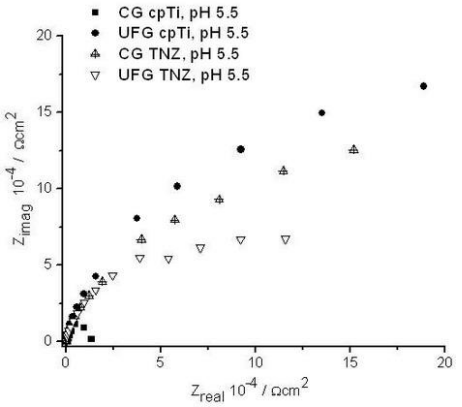

Fig. 5 The Nyquist plots of the examined materials

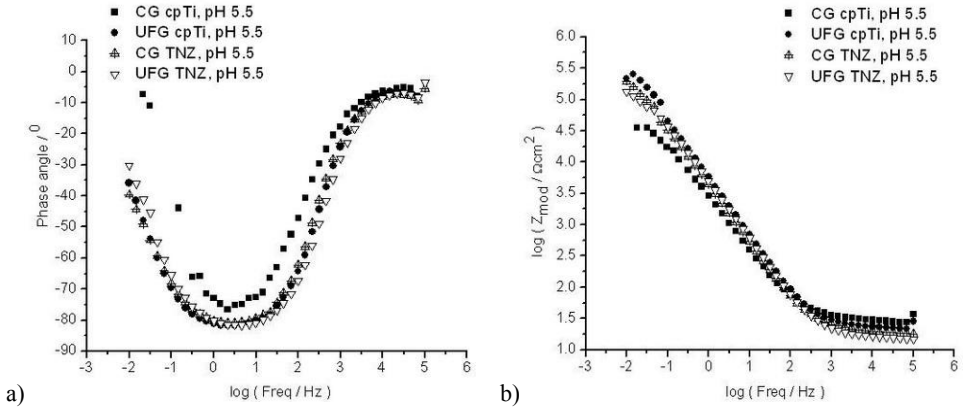

a) b)

Fig. 6 The Bode phase angle diagrams (a) and Bode modulus diagrams (b) for examined materials

The fitting results for all analyzed samples are shown in Table 2. As can be seen, the resistances of the inner barrier layers, R_2, are three orders of magnitude greater than the resistances of the outer porous layers, R_1, indicating better protective properties of the compact barrier layer. *C*PE1 and *C*PE2 represent the capacitance of the inner barrier layer and porous outer layer, respectively. CPE element is also characterized by coefficient n, which could have values between 0 and 1. When $n = 0$, the system is an ideal resistor and when $n = 1$, it is an ideal capacitor. In this study n values are between 0.82 and 0.99. CPE decreases with increasing the oxide film thickness [12]:

$$CPE=\varepsilon_0\varepsilon S/d \qquad (2)$$

where d is thickness of the oxide film, S is surface area, ε_0 is vacuum permittivity (8.854×10^{-14}Fcm^{-1}), ε is dielectric constant. The commercially pure titanium after HPT process and alloy before HPT process have a greater oxide film thickness than their counterpart.

Table 2. The electrochemical parameters extracted from EIS data

Material	R_s / Ω	R_1 / Ω cm^2	CPE$_1$		$R_2/10^3$ Ω cm^2	CPE$_2$	
			$Y_o\cdot 10^6$/ $s^n\Omega^{-1}$ cm^{-2}	n		$Y_o\cdot 10^6$/ $s^n\Omega^{-1}$ cm^{-2}	n
CG cpTi	30.3	44.2	21.5	0.91	94.9	30.6	0.89
UFG cpTi	20.0	40.7	36.0	0.87	441	21.8	0.91
CG TNZ	23.9	162	38.2	0.90	247	0.816	0.82
UFG TNZ	17.4	915	31.4	0.88	149	14.9	0.99

The EIS results show that HPT process preformed on the cpTi, leads to significant increase in corrosion resistance compared to its counterpart, which is not the case with TNZ alloy. Corrosion resistance of the metal biomaterial depends on the material composition and sample dimensions, as well as on the type, composition, temperature, pH value and volume of testing solution. Balyanov at al. [13] investigated the corrosion reistance of cpTi with both UFG and CG microstructures. In that study, they found that UFG cpTi had better corrosion resistance than CG cpTi and believed that this happened due to rapid passivation of UFG materials. On the other hand, H.Maleki-Ghaleh et al. [14] believed that the difference between corrosion behavior of CG and UFG cpTi may be related to the volume fraction of grain boundaries. Balakrishnan at al. [15] analyzed the corrosion behaviour UFG cpTi produced by equal channel angular process (ECAP) in simulated body fluid (SBF). The studies showed the corrosion resistance of the UFG cpTi to be 10 times higher compared to coarse-grained (CG) cpTi. Contrary to this, Nie et al. [16] showed that the corrosion resistance of UFG cpTi is lower than for the annealed CG cpTi. These contradictory results can be explained by a variable activity of atoms on the surface material. The corrosion resistance of UFG materials will be decreased if corrosion products are dissoluble.

4. Conclusion

In this study high pressure torsion process was used to produce ultrafine-grained cpTi and TNZ. Subsequently, electrochemical behavior of cpTi (CG and UFG) and TNZ (CG and UFG) was evaluated. The obtained results indicate that HPT process significantly reduced the grain size. Furthermore, UFG cpTi produced by HPT has better corrosion resistance compared to CG cpTi, while UFG TNZ produced by HPT has slightly lower corrosion resistance compared to CG TNZ. These contradictory results can be explained by a variable activity of atoms on the surface material. Further examinations will include electrochemical testing of these CG and UFG materials in different testing conditions (different pH values of artificial saliva, presence of lactic acid and fluoride, etc.) and with different electrochemical methods, in order to prediction behavior of these materials.

Acknowledgment

The authors acknowledge the support of the Ministry of Education, Science and Technological Development of the Republic of Serbia through the projects ON 174004 and III 45019.

Reference

[1] Kim, H. S., Kim, W. J., 2014, Annealing Effects on the Corrosion Resistance of Ultrafine-Grained Pure Titanium, Corrosion Science. 89, 331-337.

[2] Souza, M. E. P.; Lima, L.,Lima, C. R. P., Zavaglia, C.A.C., Freire, C. M. A., 2009, Effects of pH on the Electrochemical Behavior of Titanium Alloys for Implant Applications, Journal of Materials Science: Materials in Medicine 20, 549-552.

[3] S.Miran, 2014, Severe Plastic Deformation Methods to Achieve Nanostructured Materials, International Journal of Material Science 4, 98-103.

[4] A.P. Zhilyaev, T.G. Langdon, 2008, Using High-Pressure Torsion for Metal Processing: Fundamentals and Applications, Progress in Materials Science 53, 893-979.

[5] H. Yilmazer, M. Niinomi, M. Nakai, K. Cho, J. Hieda, Y. Todaka, T. Miyazaki, 2013, Mechanical Properties of a Medical β-type Titanium Alloy with Specific Microstructural Evolution Through High-Pressure Torsion, Material Science and Engineering C 33, 2499–2507.

[6] R.Z. Valiev, R.K. Islamgaliev, I.V. Alexandrov, 2000, Bulk Nanostructured Materials from Severe Plastic Deformation, Progess in Material and Science 45, 103-189.

[7] H.Y. Kim, T. Sasaki, K. Okutsu, I.J. Kim, T. Inamura, H. Hosoda, S. Miyazaki, 2006, Texture and Shape Memory Behavior of Ti-22Nb-6Ta Alloy, Acta Materialia 54, 423-433

[8] I. Dimić, I. Cvijović-Alagić, B. Völker, A. Hohenwarter, R. Pippan, Đ. Veljović, M. Rakin, B. Bugarski, 2016, Microstructure and Metallic Ion Release of Pure Titanium and Ti–13Nb–13Zr Alloy Processed by High Pressure Torsion, Materials and Design 91, 340–347.

[9] K. Sharman, P. Bazarnik, T. Brynk, A.G. Bulutsuz, M. Lewandowska, Y. Huang, T.G. Langdon, 2015, Enhancement in Mechanical Properties of a β- Titanium Alloy by High-Pressure Torsion, Journal of Materials Research and Technology 4, 79–83.

[10] K. Ozaltin, A. Panigrahi, W. Chrominski, A.G. Bulutsuz, M. Kulczyk, M.J. Zehetbauer, M. Lewandowska, 2017, Microstructure and Texture Evolutions of Biomedical Ti-13Nb-13Zr Alloy Processed by Hydrostatic Extrusion, Metallurgical and Materials Transactions AA 48, 5747-5755.

[11] A. Balakrishnan, B.C. Lee, T.N. Kim, B.B. Panigrahi, 2008, Corrosion behavior of Ultra Fine Grained Titanium in Simulated Body Fluid for Implant Application, Trends in Biomaterials and Artificial Organs 22, 58-64.

[12] I. Dimić, I. Cvijović-Alagić, A. Hohenwarter, R. Pippan,V. Kojić, J. Bajat, M. Rakin, 2017, Electrochemical and Biocompatibility Examinations of High-Pressure Torsion Processed Titanium and Ti–13Nb–13Zr Alloy, Journal of Biomedical Material Research B 00B, 1-11.

[13] A. Balyanov, J. Kutnyakova, N.A. Amirkhanova, V.V. Stolyarov, R.Z. Valiev, X.Z. Liao, Y.H. Zhao, Y.B. Jiang, H.F. Xu, T.C.Lowe, Y.T. Zhu, 2004, Corrosion Resistance of Ultra Fine-Grained Ti, Scripta Material 51, 225–229.

[14] H.Maleki-Ghaleh, K. Hajizadeh, A. Hadjizadeh, M.S. Shakeri, S. Ghobadi Alamdari, S. Masoudfar, E. Aghaie, M. Javidi, J. Zdunek, K.J. Kurzydlowski, 2014, Electrochemical and Cellular Behavior of Ultrafine-Grained Titanium in Vitro, Material Science and Engineering C 39, 299–304.

[15] A. Balakrishnana, B.C. Leea, T.N. Kima and B.B. Panigrahib, 2008, Corrosion Behaviour of Ultra Fine Grained Titanium in Simulated Body Fluid for Implant Application,Trends in Biomaterial and Artificial Organs 22 58-64.

[16] M. Nie, C.T. Wang, M. Qu, N. Gao, J.A. Wharton, T.G. Langdon, 2014, The Corrosion Behaviour of Commercial Purity Titanium Processed by High-Pressure Torsion, Journal of Material Science 49, 2824–2831.